UNIVERSITY OF WEST BOHEMIA

Applied and Computational Mechanics 3 (2009) 241–252

Applied and Computational Mechanics

# Modelling of the three-dimensional friction contact of vibrating elastic bodies with rough surfaces

J. Voldřich[a,*]

[a] *New Technologies Research Centre, University of West Bohemia, Univerzitní 8, 306 14 Plzeň, Czech Republic*

Received 5 September 2008; received in revised form 6 November 2008

**Abstract**

Friction contact appears to be an intricate nonlinear coupling in modelling engineering structures. With vibration systems, it can serve as a dampening element for reducing the stress range. The contribution deals with the modelling of the 3D dry friction elastic contact. The influence of surface roughness on its normal and tangential stiffness, both of nonlinear nature, is being considered. The model also allows a change of the normal contact force and of the applied moment of force in the course of a vibration cycle. The equations of the proposed mathematical model have been solved using direct integration.


*Keywords:* contact model, friction oscillator, vibration

## 1. Introduction

The friction in the mechanical systems is often a welcome effect or, even, it determines the functionality of a device. By way of example, we can mention vehicle disk and shoe brakes or friction clutches. An important part of some vibrating systems are friction dampers. The largest of them form part of many buildings in seismic active areas. From the point of view of the mathematical modelling, an extraordinary attention has been given to the friction dampers in bladed disk assemblies of the gas and steam turbines. A nonhomogenous stream of the medium within these mechines causes the high-frequency vibrations. Excessive amplitudes can be responsible for high cycle fatigue failures. The role of the friction dampers and shroud contacts is to cut down the level of the vibrations or to re-tune the resonance frequencies [1, 4, 5, 11, 12]. The dry friction damping concept in gas turbines lies in principle in a metal piece loaded by centrifugal force against the underside of the platforms of two adjacent blades [5, 13]. Still is of course very difficult to estimate precisely the influence of this kind of damping.

The highest attention was paid to the 1D friction oscillators in connection with the friction dampers. A lot of works has been recently published which deal with their several aspects. Some of them are above all focused at the modelling of stationary vibrations caused by the external harmonic excitation. The problem has been solved particularly in the frequency area. A sufficiently exact representation of the hysteresis dissipation loop (i.e. the dependence of the applied friction force on the relative displacement of the adjacent contact surfaces), tangential stiffness of the contact, influence of the magnitude of the normal force or excitation amplitude on vibrations has been particularly stressed [6]. Other works treating

*Corresponding author. Tel.: +420 377 634 734, e-mail: voldrich@ntc.zcu.cz.

1D friction oscillators are concentrated on precise covering of the stick, slip, and, as the case may be, separation, and investigate also bifurcation phenomena that lead for example to different number of transients stick-slip during one cycle [7, 8]. In most cases, the solution of the mathematical model with respect to the time using direct integration is replaced by a solution with respect to the frequency by applying a quasi-linearization technique. The mostly often used is Harmonic Balance Method (HBM) [5, 11] or multi-HBM if the case is a little more sophisticated excitation or the necessity to pay regard to number of eigenvectors of the mechanical system. In such a case or in case with a number of degrees of freedom, the mentioned methodology lies in a transformation of nonlinear differential equations into a set of nonlinear algebraic equations. The methodology of the solution with respect to the frequency is preferred as it is computationally less demanding. Even the suggestions of the frequency-time methods for the vibration dry-friction-damped systems can be encountered in isolated instances [2, 9, 10].

It is the actual gas turbine friction dampers range of problems that illustrates that the 1D friction coupling is too limiting and that the relative motion of the contact selected point against the opposite surface is adequate to describe at any rate by an ellipse-like curve [1, 11, 13]. Equally the macroslip model of the contact consisting in putting the point contact in place of the complex contact must not be sufficient. In other words one part of the real contact can be in the stick phase while the other in the slip phase and this two-facedness can change the general characteristics of the hysteresis dissipation loop [6]. This is the reason why the so called microslip models are developed [5]. The range of issues of frictionally constrained 3-DOF oscillators was solved rather exceptionally in [3, 14, 15, 16], where even a variation of the applied overall normal force in the course of the vibration cycle has been assumed. It should be however noted that even the very coverage of the normal force change must not be sufficient in case of the shroud contacts in turbines blades. What is more, the snag is that even the moment of force acting between the contact surfaces can vary thus making the normal contact pressure different at different contact points and can undergo changes in the course of a cycle if the torsional vibrations of the blades are rather intense. The authors have a feeling that practically no attention has been given to this problem in the relevant literature. From the point of view of the mathematical modelling, one more inconvenience occurs when the contact coupling is preloaded insufficiently or when at least a part of the contact is nearing to the transition to the phase of separation under influence of the normal pressure change. In such a case, it is advisable to include the influence of the surface roughness which manifests itself by the nonlinear both of normal and tangential contact stiffnesses [14].

The presented work deals with computer aided modelling of the friction contact seen as a nonlinear coupling in the mechanical systems with small vibrations. Its goal is describing the procedure that includes both the influence of the surface roughness on the contact stiffness (in analogy to [14]) and its 3D kinematics, and the change of the normal force and momentum during a vibration cycle. The associated differential equations are solved with respect to the time variable as the transients between the stick, slip, and separation phases respectively are watched closely. Following paragraph is devoted to the actual description of the stiffness and of the general model of the friction contact. The third paragraph introduces this nonlinear coupling as a part of the description of the general vibration dynamical system. Finally, the paragraphs 4 presents some examples of the numerical results partly to illustrate the proposed methodology. In order to familiarize better with problems in question, the attention is paid at first to the 1D friction oscillator while a variation of the applied normal force is the subject in what follows.

## 2. Friction contact model

### 2.1. Contact stiffnesses of rough surfaces

Let us consider a plane elastic foundation, the contact surface of which will be divided into rectangular area elements with dimensions $h$ and $b$. Thus we obtain a nominal contact surface $S = hb$. Further, the length $d$ describes the length of the undeformed elastic foundation in the normal direction. If the surface is ideally planar, the nominal normal stiffness of the corresponding element is $k_N = \hat{E}S/d$, while the tangential stiffness is $k_T = \hat{G}S/d$. Here $\hat{E}$ denotes a generalized modulus of elasticity while $\hat{G}$ is a generalized shear modulus of elasticity. Let us further consider a rough surface to which an ideal planar stiff plate has been applied. Let us introduce a coordinate system the origin of which lies on the surface of the plate and the axes $y$ a $z$ are parallel to the rectangular element sides. Let us put a parallel plane at a distance of $x$ from this stiff plate that however intersects the rough surface (see fig. 1) at an area of not $hb$ but only $\vartheta(x)b$ size. Let us denote $R$ the quantity characterizing the surface roughness. Let us next introduce dimensionless quantities $h^* = \vartheta/h$ and $x^* = x/R$. An approximation

$$h^*(x^*) = \begin{cases} 0 & \text{for } x^* < 0\,, \\ 3x^{*2} - 2x^{*3} & \text{for } 0 \le x^* \le 1\,, \\ 1 & \text{for } x^* > 1\,. \end{cases} \tag{1}$$

is proposed in [14]. This situation can be covered rather faithfully by means of the Gauss distribution that corresponds most exactly to the measurements of the roughness but it is more demanding from the computational point of view. Let $u$ denotes displacement (deformation) of an element in the normal direction $x$, $F_N$ applied normal contact force acting on the element area $S$, and $F_{Ty}$, $F_{Tz}$ components of applied tangential force. The corresponding dimensionless quantities will then be

$$u^* = \frac{u}{R}\,, \quad F_N^* = \frac{F_N}{k_N R}\,, \quad F_{Ty}^* = \frac{F_{Ty}}{k_T R}\,, \quad F_{Tz}^* = \frac{F_{Tz}}{k_T R}\,.$$

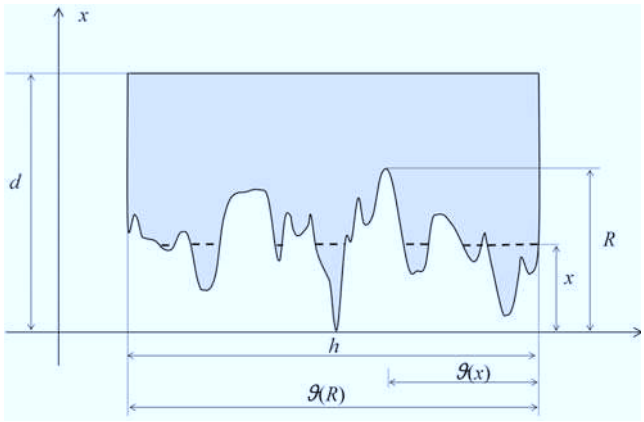


Fig. 1. Rough surface with a parallel section at a distance of $x$. The length of the section is $\vartheta(x)$

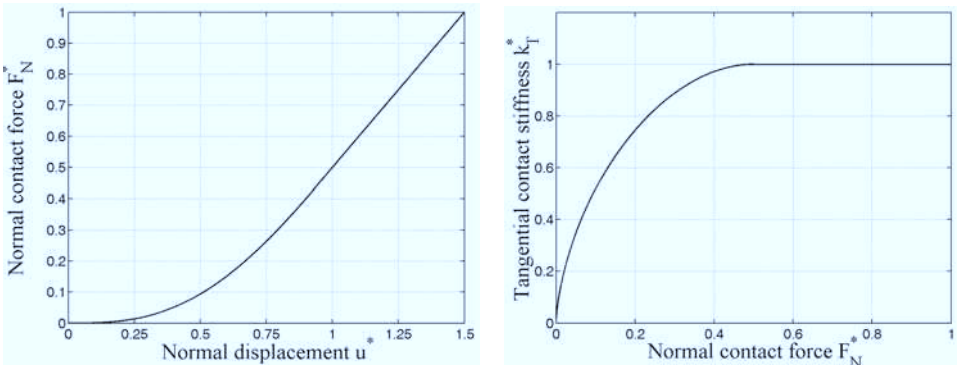


Fig. 2. Normal force-displacement relationship and tangential contact stiffnesses versus normal force

Now it is possible to derive (see e.g. [14])

$$F_N^*(u^*) = \begin{cases} 0 & \text{for } u^* \leq 0\,, \\ u^{*3} - \frac{1}{2}u^{*4} & \text{for } 0 \leq u^* \leq 1\,, \\ u^* - \frac{1}{2} & \text{for } u^* > 1\,, \end{cases} \tag{2}$$

for $F_N^*$ as a function of $u^*$ from the variation of the function $h^*$ defined by the formula (1). For the tangential component of the force (in the direction $z$) we can write $F_{Tz} = \frac{k_T}{S} b\vartheta w = k_T h^* w = \overline{k}_T w$, where $w$ denotes the corresponding tangential displacement. The dimensionless tangential stiffness $k_T^* = \overline{k}_T / k_T = h^* = h^*(u^*)$ is therefore a function of the acting normal force (see fig. 2).

The mutual contact of two rough surfaces can be modelled as a contact of one rough surface with a smooth rigid wall. In such a case it is necessary to take into consideration the nominal quantities $R$, $k_N$ a $k_T$ according to the relations

$$R = \sqrt{R_1^2 + R_2^2}, \quad \frac{1}{k_N} = \frac{1}{k_{N1}} + \frac{1}{k_{N2}}, \quad \frac{1}{k_T} = \frac{1}{k_{T1}} + \frac{1}{k_{T2}},$$

where $R_i$, $k_{Ni}$, $k_{Ti}$, $i = 1, 2$, are nominal quantities of individual surfaces.

### *2.2. Point contact element*

Let us consider a contact between small surfaces with a size of $S = hb$. The constrained force consists of two components. The first one is the induced friction force on the contact plane while the other is the variable normal force. Since the friction force is fully characterized by a relative motion of the contact surfaces, it will not lose generality to assume one of the contacting surfaces is the ground for this moment. Let us assume that the contact is preloaded by a normal force $F_{N0}$. A normal force acting at the time point $t$ will then have a magnitude of $F_N(t)$. For the following, let us denote tangential contact force by $\mathbf{F_T} = [0, F_{Ty}, F_{Tz}]^T$, the input tangential relative motion $\mathbf{v} = [0, v, w]^T$, the slip motion of the contact point $\mathbf{v_s} = [0, v_s, w_s]^T$. Let us further denote the deformation corresponding to the magnitude of the preloading normal force $F_{N0}$ as $u_0$, the deformation corresponding to the magnitude of the force $F_N$ by $u$.

Depending on the amplitude and phase of the vibration motion components, the friction contact will either be stick, slip or separate during a cycle of oscillation. Taking into account

the Coulomb friction law, the conditions for the above mentioned states can be expressed as follows.

$$\text{Stick condition:} \qquad |\mathbf{F_T}| = |\overline{k}_T(F_N)(\mathbf{v}-\mathbf{v_0})| < \mu F_N\,, \quad \dot{\mathbf{v}}_\mathbf{s} = 0\,; \tag{3}$$

$$\text{Slip condition:} \qquad \mathbf{F_T} = \mu F_N \frac{\dot{\mathbf{v}}_\mathbf{s}}{|\dot{\mathbf{v}}_\mathbf{s}|}\,, \quad \dot{\mathbf{v}}_\mathbf{s} \neq 0\,; \tag{4}$$

$$\text{Separation condition:} \qquad F_N = 0\,. \tag{5}$$

Here $\mathbf{v_0}$ is an initial value of $\mathbf{v}$ at the beginning of the stick state, and $\mu$ means a friction coefficient. If the real contact is the case, the coefficient alone is generally dependent on the slippage rate. Most commonly, this dependence is declared by the relationships

$$\mu = (\mu_0 - \mu_\infty)\, e^{-\lambda|\dot{\mathbf{v}}_\mathbf{s}|} + \mu_\infty \quad \text{or} \quad \mu = \frac{\mu_0}{1 + p|\dot{\mathbf{v}}_\mathbf{s}|}\,,$$

where $\mu_0$ is a static friction coefficient and $\mu_\infty$, $\lambda$, $p$ are some additional material parameters of the contact.

In case of very small vibration amplitudes, when the contact does not slip, only elastic deformations occur and, consequently, no energy is dissipated due to the contact. This however is not true when the slip occurs. The amount of the dissipated energy is defined by the nature of the hysteresis loop (see fig. 3).

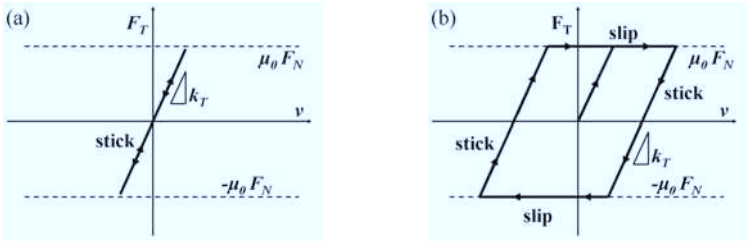


Fig. 3. Friction force versus relative motion. (a) Only the stick state occurs, (b) Hysteresis loop if the quantities $\mu$ and $F_N$ remain constant

### *2.3. Contact area model*

It is often questionable to model the contact coupling of real mechanical systems in terms of a point element. Let us give further consideration to a planar rectangular contact with centres $O_{(1)}$ and $O_{(2)}$ of both surfaces. These points are identical in the equilibrium state and $O \equiv O_{(1)} \equiv O_{(2)}$. So as to be able to describe the vibrations of the mechanical system with this contact coupling as a whole we will investigate the local displacements and rotations

$$\mathfrak{u}_{(k)} = [u_{(k)}, v_{(k)}, w_{(k)}, \varphi_{x(k)}, \varphi_{y(k)}, \varphi_{z(k)}]^T \in \mathbb{R}^6\,,\ k = 1, 2, \tag{6}$$

of the points $O_{(k)}$, and also an overall force $\mathfrak{F} = [F_N, F_{Ty}, F_{Tz}]^T$ and a moment of force $\mathfrak{M} = [M_x, M_y, M_z]^T$ due to the contact. The quantities describing the static preloading will be

$$\mathfrak{u}_{0(k)} = [u_{0(k)}, 0, 0, 0, \varphi_{y0(k)}, \varphi_{z0(k)}]^T\,, \quad \mathfrak{F}_0 = [F_{N0}, 0, 0]^T\,, \quad \mathfrak{M}_0 = [0, M_{y0}, M_{z0}]^T\,.$$

Here $(x, y, z)$ denotes a local coordinate system centred at the point $O$. The axis $x$ is perpendicular to either surface, the orientation of the axes $y$ and $z$ is visualized in the fig. 4. Let

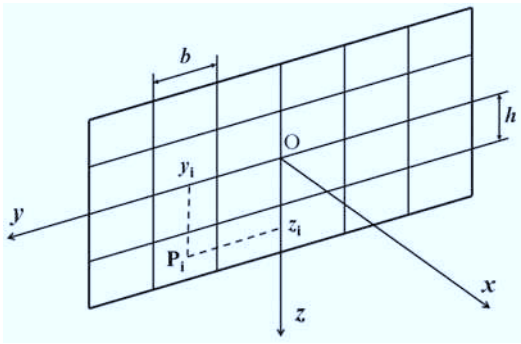


Fig. 4. Contact area with subregions

us subdivide the considered contact surface into $n \cdot m$ pairs of rectangular subregions. We model the contact condition between each pair with the aid of a point contact element which we have described in the previous paragraph. For the i-th pair of the subregions, let us denote the corresponding quantities defining the contact conditions by adding the subscript $i$, i.e. $u_{0i}$, $\mathbf{u_i} = [u_i, v_i, w_i]^T$, $F_{N0i}$, $\mathbf{F_i} = [F_{Ni}, F_{Tyi}, F_{Tzi}]^T$. We denote the position vector of the centre $P_i$ of the i-th pair expressed using the local coordinates of the system with $\mathbf{r_i} = [0, y_i, z_i]^T$. The relationships among the quantities of the contact total balance at its centre $O$ and the quantities of the point elements in $P_i$ then will be

$$\mathbf{u_i} = \mathbf{G_i}\,(\mathfrak{u}_{(2)} - \mathfrak{u}_{(1)})^T \quad \text{with} \quad \mathbf{G_i} = \begin{pmatrix} 1 & 0 & 0 & 0 & z_i & -y_i \\ 0 & 1 & 0 & -z_i & 0 & 0 \\ 0 & 0 & 1 & y_i & 0 & 0 \end{pmatrix}, \tag{7}$$

$$\mathfrak{F} = \sum_{i=1}^{n.m} \mathbf{F_i}\,, \quad \mathfrak{M} = \sum_{i=1}^{n.m} \mathbf{r_i} \times \mathbf{F_i}\,. \tag{8}$$

## 3. Equations of motion

We will model the vibrations of the mechanical system as a whole in terms of the equations of motion in the form

$$\mathbf{M}\ddot{\mathbf{x}}(t) + \mathbf{B}\dot{\mathbf{x}}(t) + \mathbf{K}\mathbf{x}(t) + \mathbf{f_N}(\mathbf{x}(t), \mathfrak{F}_0, \mathfrak{M}_0) = \mathbf{f}(t)\,, \tag{9}$$

where $\mathbf{M}$, $\mathbf{B} = \alpha\mathbf{I} + \beta\mathbf{K}$, $\mathbf{K} \in \mathbb{R}^{r,r}$ are matrices of mass, damping and stiffness, respectively, and $\mathbf{f_N}$, $\mathbf{f} \in \mathbb{R}^r$ are vector of nonlinear contacts generalized forces and vector of external excitation, respectively. Vector $\mathbf{x} \in \mathbb{R}^r$ of vibration physical displacements and rotations also includes the displacements and rotations at the nodes $O_{(1)}, O_{(2)}$ of the nonlinear contact couplings, that is

$$\mathbf{x} = [\ldots, \mathfrak{u}_{(1)} - \mathfrak{u}_{0(1)}, \mathfrak{u}_{(2)} - \mathfrak{u}_{0(2)}, \ldots]^T\,. \tag{10}$$

Similarly, for the vector of generalized forces, we have

$$\mathbf{f_N} = [\ldots, -\mathfrak{F} + \mathfrak{F}_0, -\mathfrak{M} + \mathfrak{M}_0, \mathfrak{F} - \mathfrak{F}_0, \mathfrak{M} - \mathfrak{M}_0, \ldots]^T\,. \tag{11}$$

The number of degrees of freedom (DOF) $r$ can be rather appreciable in case of real mechanical systems. It is therefore purposeful to reduce it using the modal transformation

$$\mathbf{x}(t) = \mathbf{\Phi}\mathbf{q}(t)\,, \tag{12}$$

where $\mathbf{\Phi} = [\phi_1, \ldots, \phi_s] \in \mathbb{R}^{r,s}$ is a matrix composed of the eigenvectors $\phi_i$, $i = 1, \ldots, s$ of the eigenvalue problem $(\mathbf{K} - \lambda\mathbf{M})\phi = \mathbf{0}$ with $\mathbf{\Phi}^T\mathbf{M}\mathbf{\Phi} = \mathbf{I}$, $\mathbf{\Phi}^T\mathbf{K}\mathbf{\Phi} = \mathbf{\Lambda}$, $\mathbf{\Phi}^T\mathbf{B}\mathbf{\Phi} = \alpha\mathbf{I} + \beta\mathbf{\Lambda}$ with $\mathbf{\Lambda} = diag(\omega_1^2, \ldots, \omega_s^2)$. Here $\omega_i$ denotes $i$-th natural frequency of a mechanical system free of any coupling. The new vector of modal coordinates $\mathbf{q}(t)$ is an element of the new configuration space of dimension $s \ll r$. The problem (9) becomes thus transformed into the form

$$\ddot{\mathbf{q}}(t) + (\alpha\mathbf{I} + \beta\mathbf{\Lambda})\dot{\mathbf{q}}(t) + \mathbf{\Lambda}\mathbf{q}(t) + \mathbf{\Phi}^T\mathbf{f_N}(\mathbf{\Phi}\mathbf{q}(t), \mathfrak{F}_0, \mathfrak{M}_0) = \mathbf{\Phi}^T\mathbf{f}(t) \tag{13}$$

The solution (13) will be found by means of the direct integration in such a way that after some standard operations we convert (13) into a system of differential equations of the first order and apply the Runge-Kutta method of the fourth order. The calculation of the vector $\mathbf{f_N}$ of the contact forces and moments is being performed in the following steps:

- given $\mathbf{q}(t)$ at the time point $t$,
- establishing $\mathfrak{u}_{(1)}$, $\mathfrak{u}_{(2)}$ according to (12) and (10),
- calculation $\mathbf{u}_i$, $i = 1, \ldots, nm$, according to (7),
- calculation $\mathbf{F}_i$, $i = 1, \ldots, nm$, using the relationships (2), (3), (4),
- calculation $\mathfrak{F}$, $\mathfrak{M}$ according to the relationships (8),
- establishing $\mathbf{f_N}$ according to (11),
- calculation $\mathbf{q}(t + \Delta t)$ by solving (13) with time step $\Delta t$.

## 4. Numerical examples of friction contacts

### *4.1. 1-DOF friction oscillators*

A friction oscillator with one degree of freedom and outer harmonic excitation $A\sin(\Omega t)$ is displayed in the fig. 5. The natural frequency of an oscillator without friction coupling is $\omega_0 = \sqrt{c/m}$, where $m$ is mass, $c$ spring constant, the damping ratio is $b$. Let us furthermore consider a constant normal force $F_{N0}$ and a constant friction coefficient $\mu_0$. Using the normalized time $\tau = \omega_0 t$, $(.)' = \dfrac{d}{d\tau} = \dfrac{1}{\omega_0}\dfrac{d}{dt}$, and the damping ratio $D = b/2\sqrt{mc}$ as well as the frequency ratio $\eta = \Omega/\omega_0$ the problem of oscillations can be described by the equation

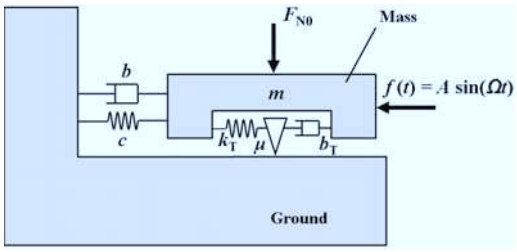


Fig. 5. Scheme of a 1-DOF friction oscillator.

$$v''(\tau) + 2Dv'(\tau) + v(\tau) + \begin{cases} \dfrac{k_T}{c}\, k_T^* \,(v - v_0) & (stick) \\ \dfrac{\mu_0\, F_{N0}}{A}\, \mathrm{sign}(v) & (slip) \end{cases} = \sin(\eta\tau)\,, \tag{14}$$

where $v = \dfrac{c}{A} y$ is a normalized displacement. As a rule, $c \ll k_T$, $k_T^* = 1$ holds often in real technical systems and the dimensionless parameters $\mu_0 F_{N0}/A$ as well as the frequency ratio $\eta$ make the decision as to the character of the vibrations. The fig. 6 shows the solutions of the equation (14) with $\eta = 0.75$, $0.5$, $0.25$ and $0.15$ respectively for the values $D = 0.05$, $k_T/c = 100$, $k_T^* = 1$ a $\mu_0 F_{N0}/A = 0.5$. It is easily seen that a slip occurs in the whole course of the vibration cycle for the value $\eta = 0.75$. If $\eta = 0.5$ and $0.25$ the stick stage occurs during the cycle, with $\eta = 0.15$ the phases stick and slip take turns four times.

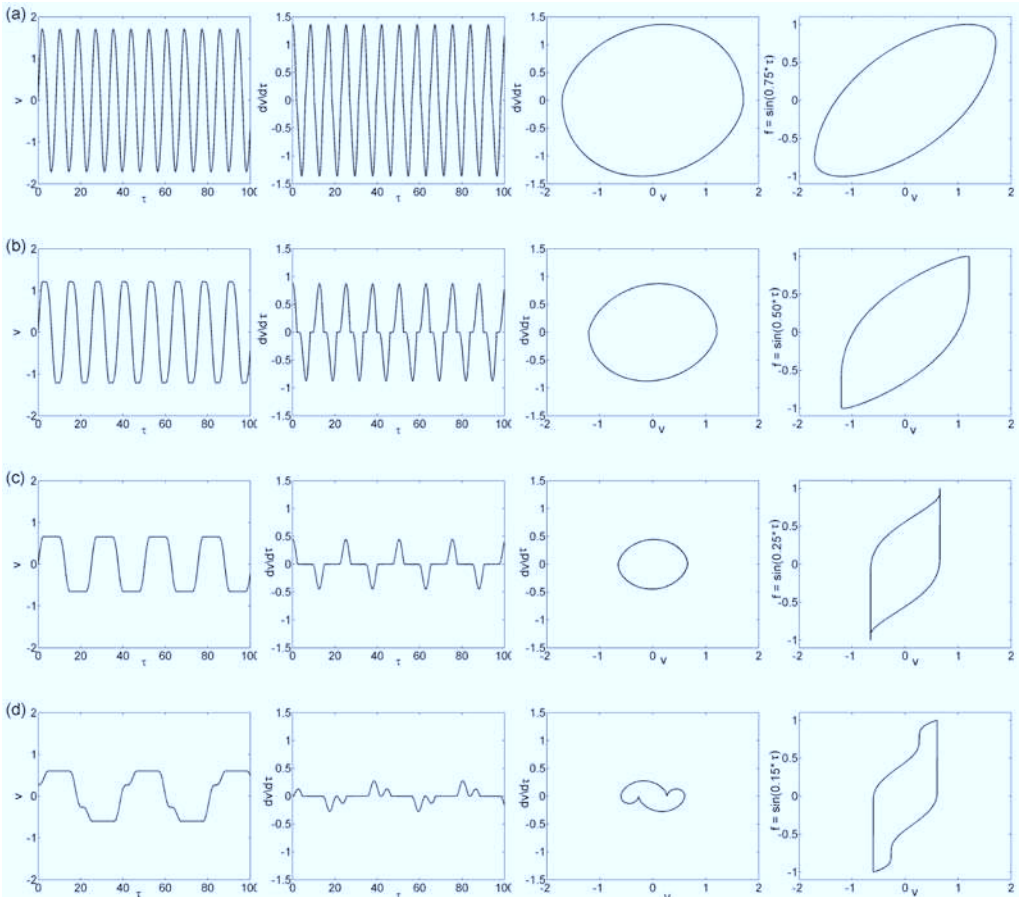


Fig. 6. Solution of normalized equation (14) illustrated by the graphs $\tau - v(\tau)$, $\tau - dv(\tau)/d\tau$, $v(\tau) - dv(\tau)/d\tau$ and $v(\tau) - \sin(\eta\tau)$ for the parameters values $\mu_0 F_{N0}/A = 0.5$ and $k_T/c = 100$. (a) $\eta = 0.75$, (b) $\eta = 0.50$, (c) $\eta = 0.25$, (d) $\eta = 0.15$

### 4.2. Example 2

In the first place, let us investigate the response of 2-DOF system depicted in the fig. 7 with displacements of the mass $m1$ and $m2$ in the direction $y$. The values of the masses are $m1 = 1\,\text{kg}$, $m2 = 1\,\text{kg}$ and of stiffnesses $c1 = 41\,339\,\text{N/m}$, $c2 = 41\,328\,\text{N/m}$. Then we have eigenfrequencies 20 Hz and 52.4 Hz if we omit the friction contact. The corresponding eigenvectors are

$$(0.525\,7, 0.850\,7)^T, \quad (-0.850\,7, 0.525\,7)^T. \tag{15}$$

Further $k_T = 40\,000\,\text{N/m}$, $\mu = 0.5$, the value of the specific ratio of damping coefficient is 0.02. A harmonic excitation in the direction $y$ with an amplitude of $A = 10\,\text{N}$ acts on the mass point $m2$. The excitation frequency varies between 18 Hz and 28 Hz. The frequency dependencies of the responses for different values of the preloading force of $F_{N0} = 0$, 10 N, 20 N, 30 N, 50 N, 100 N, 200 N and 600 N are shown in the fig. 8. It is obvious, that we can reach a markedly lower responce than for the system without the friction contact or for the situation when no slip accurs in the contact. The preloading value $F_{N0} = 30\,\text{N}$ seems the best one. It is useful to notice that the maximum of the graphs for the free and stuck states is greater than responces of any other state.

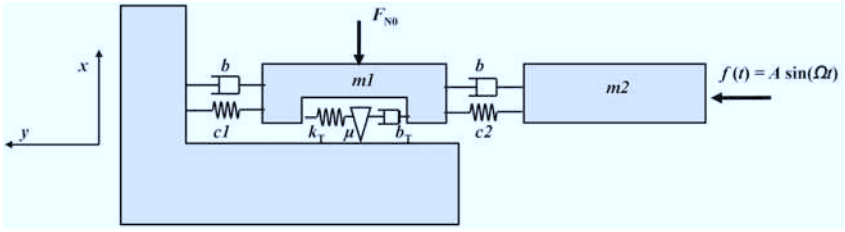


Fig. 7. Scheme of a 2-DOF system with friction contact

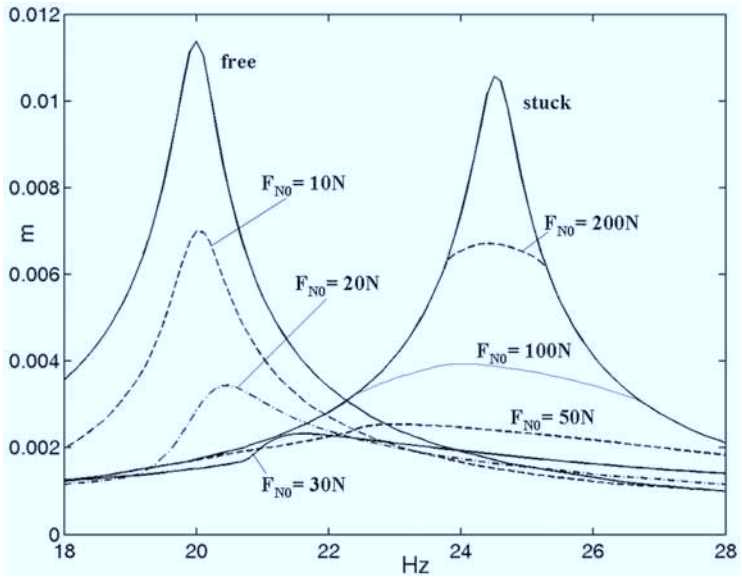


Fig. 8. Frequency responce of 2-DOF system with friction contact for different values of the preloading force $F_{N0}$

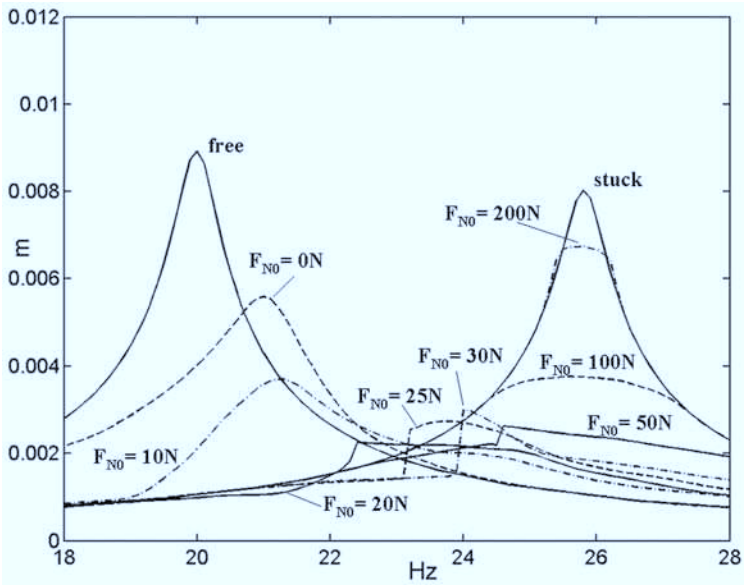


Fig. 9. Frequency responce of coupling system with friction contact for different values of the preloading force $F_{N0}$

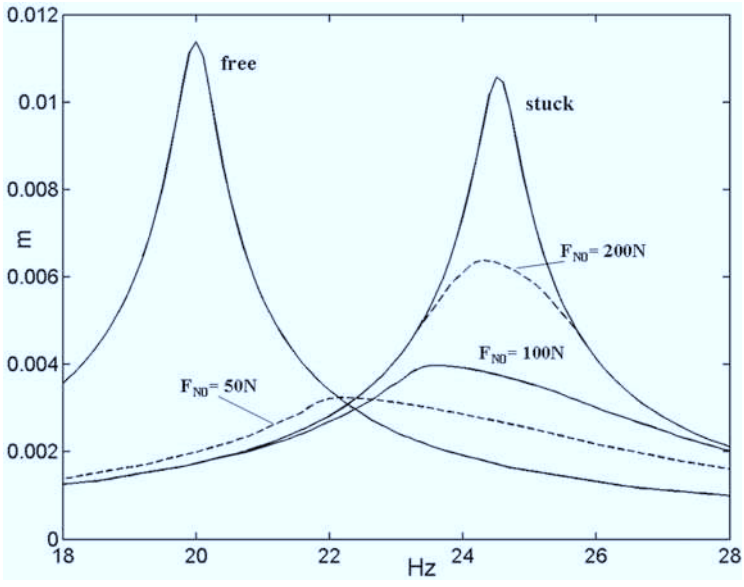


Fig. 10. Frequency responce of 2-DOF system with friction contact for the preloading moment of force $M_{y0} = 1\,\mathrm{Nm}$

The spatial behaviour of a vibrating system will manifest itself if we add the displacement of the mass $m1$ in the direction $x$ (i.e. in the normal direction to the contact plane) as the new DOF. Overall, we carry out only one modification of input values for the equation (13) and substitute the first eigenvector from (15) by a new eigenvector

$$(0.46531, 0.46531, 0.752975)^T, \quad (0., -0.8507, 0.5257)^T .$$

(Of course, the scheme from the fig. 7 and values $m1$, $m2$, $c1$, $c2$ need not be preserved.) The corresponding results are presented in the fig. 9. It can be seen that a little more substantial differences occur especially for preloading values $F_{N0}$ from 10 N to 100 N. We can also see that the maximum of the graphs of free and stuck states is not any more a sufficient estimate for responces with another preloading values $F_{N0}$. The jumps within graphs with $F_{N0} = 25$ N, 30 N and 50 N relate to bifurcation phenomena.

Similarly the effect of the preloading moment of force $\mathfrak{M}_0$ can be studied. Let us return to the first example from the fig. 7 with two DOFs. The results for the first eigenvector of (15) and for the value $M_{y0} = 1$ Nm (see the subsection 2.3) are presented in the fig. 10. Dimensions of the contact area are $h = b = 0.1$ m with 16 subregions ($n = m = 4$). We can see the higher responce for the preloading force $F_{N0} = 50$ N as against the situation from fig. 8.

## 5. Conclusion

The work deals with modelling of the friction contact in the mechanical systems with small vibrations. The influence of the surface roughness on the contact stiffness is described and the change of the normal contact force and moment during a vibration cycle is considered. Two examples of simple mechanical systems are presented at least partly to illustrate the proposed methodology. The effect of the change of the normal force and of the preloading moment of force are given in the fig. 8, 9 and 10, where the frequency responces of the second system (see fig. 7) are depicted. The results show that phenomena with normal contact forces could not be omitted if accurate conclusions are required.

## Acknowledgements

The paper is based on work supported by the Czech Ministry of Education under the research project 1M06059.

## References

[1] C. Bréard, J. S. Green, M. Vahdati, M. Imregun, A non-linear integrated aeroelasticity method for the prediction of turbine forced response with friction dampers, International Journal of Mechanical Sciences 43 (2001) 2 715–2 736.

[2] D. Charleux, C. Gibert, F. Thouverez, J. Dupeux, Numerical and experimental study of friction damping in blade attachments of rotating bladed disks, International Journal of Rotating Machinery (2006), Article ID71302, 1–13, DOI 10.1155/IJRM/2006/71302.

[3] J. J. Chen, B. D. Yang, C. H. Menq, Periodic forced response of structures having three-dimensional frictional constraints, Journal of Sound and Vibration 229 (4) (2000) 775–792.

[4] E. Ciğeroğlu, H. N. Őzgűven, Nonlinear vibration analysis of bladed disks with dry friction dampers, Journal of Sound and Vibration 295 (3–5) (2006) 1 028–1 043.

[5] G. Csaba, Modelling Microslip Friction Damping and its Influence on Turbine Blade Vibrations, Dissertations, Linkoping University, 1998.

[6] S. Filippi, M. Gola, A. Akay, Measurement of tangential contact hysteresis during microslip, ASME Journal of Tribology 126 (3) (2004) 482–489.

[7] N. Hinrichs, M. Oestreich, K. Popp, On the modelling of friction oscillators, Journal of Sound and Vibration 216 (3) (1998) 435–459.

[8] H. K. Hong, C. S. Liu, Coulomb friction oscillator: modeling and responses to harmonic loads and base excitations, Journal of Sound and Vibration 229 (5) (2000) 1 171–1 192.

[9] D. Laxalde, F. Thouverez, J. J. Sinou, J. P. Lombard, Qualitative analysis of forced response of blisks with friction ring dampers, European Journal of Mechanics A/Solids 26 (2007) 676–687.

[10] S. Nacivet, C. Pierre, F. Thouverez, L. Jezequel, A dynamic Lagrangian frequency-time method for the vibration of dry-friction-damped systems, Journal of Sound and Vibration 265 (2003) 201–219.

[11] K. Y. Sanliturk, D. J. Ewins, Modelling two-dimensional friction contact and its application using harmonic balance method, Journal of Sound and Vibration 193 (2) (1996) 511–523.

[12] K. Y. Sanliturk, D. J. Ewins, R. Elliott, J. S. Green, Friction damper optimisation: Simulation of rainbow tests, Journal of Engineering for Gas Turbines and Power 123 (2001) 930–939.

[13] K. Y. Sanliturk, D. J. Ewins, A. B. Stanbridge, Underplatform dampers for turbine blades: Theoretical modelling, analysis and comparison with experimental data, ASME Journal of Engineering for Gas Turbines and Power 123 (2001) 919–931.

[14] W. Sextre, Dynamic Contact Problems with Friction, Springer-Verlag, Berlin, Heildelberg, 2007.

[15] B. D. Yang, M. L. Chu, C. H. Menq, Stick-slip-separation analysis and non-linear stiffness and damping characterization of friction contacts having variable normal load, Journal of Sound and Vibration 210 (4) (1998) 461–481.

[16] B. D. Yang, C. H. Menq, Characterization of 3D contact kinematics and prediction of resonant response of structures having 3D frictional constraint, Journal of Sound and Vibration 217 (5) (1998) 909–925.